The U-Box/ARM E3 Ligase PUB13 Regulates Cell Death, Defense, and Flowering Time in Arabidopsis[1][C][W][OA]

Wei Li[2], Il-Pyung Ahn[2], Yuese Ning, Chan-Ho Park, Lirong Zeng, Justin G.A. Whitehill, Haibin Lu, Qingzhen Zhao, Bo Ding, Qi Xie, Jian-Min Zhou, Liangying Dai[3], and Guo-Liang Wang[3]*

Hunan Provincial Key Laboratory of Crop Germplasm Innovation and Utilization and Hunan Provincial Key Laboratory of Biology and Control of Plant Diseases and Insect Pests, Hunan Agricultural University, Changsha, Hunan 410128, China (W.L., Y.N., L.D., G.L.W.); State Laboratory for Biology of Plant Diseases and Insect Pests, Institute of Plant Protection, Chinese Academy of Agricultural Sciences, Beijing 100193, China (Y.N., G.L.W.); Department of Plant Pathology, Ohio State University, Columbus, Ohio 43210 (W.L., I.-P.A., C.-H.P., L.Z., J.G.A.W., B.D., G.L.W.); National Institute of Biological Sciences, Beijing 102206, China (W.L., H.L., J.-M.Z.); Department of Biology, University of Arkansas, Little Rock, Arkansas 72204 (L.Z.); and State Key Laboratory of Plant Genomics, National Center for Plant Gene Research, Institute of Genetics and Developmental Biology, Chinese Academy of Sciences, Beijing 100101, China (Q.Z., Q.X.)

The components in plant signal transduction pathways are intertwined and affect each other to coordinate plant growth, development, and defenses to stresses. The role of ubiquitination in connecting these pathways, particularly plant innate immunity and flowering, is largely unknown. Here, we report the dual roles for the Arabidopsis (*Arabidopsis thaliana*) Plant U-box protein13 (PUB13) in defense and flowering time control. In vitro ubiquitination assays indicated that PUB13 is an active E3 ubiquitin ligase and that the intact U-box domain is required for the E3 ligase activity. Disruption of the *PUB13* gene by T-DNA insertion results in spontaneous cell death, the accumulation of hydrogen peroxide and salicylic acid (SA), and elevated resistance to biotrophic pathogens but increased susceptibility to necrotrophic pathogens. The cell death, hydrogen peroxide accumulation, and resistance to necrotrophic pathogens in *pub13* are enhanced when plants are pretreated with high humidity. Importantly, *pub13* also shows early flowering under middle- and long-day conditions, in which the expression of *SUPPRESSOR OF OVEREXPRESSION OF CONSTANS1* and *FLOWERING LOCUS T* is induced while *FLOWERING LOCUS C* expression is suppressed. Finally, we found that two components involved in the SA-mediated signaling pathway, SID2 and PAD4, are required for the defense and flowering-time phenotypes caused by the loss of function of PUB13. Taken together, our data demonstrate that PUB13 acts as an important node connecting SA-dependent defense signaling and flowering time regulation in Arabidopsis.

The ubiquitin/26S proteasome-mediated pathway is involved in selective degradation of proteins in cells of eukaryotic organisms. In plants, ubiquitination has been implicated in a variety of processes, including cell cycle, circadian rhythm control, hormone signaling, senescence, disease resistance, and photomorphogenesis/flowering (Jang et al., 2005; Vega-Sánchez et al., 2008; Henriques et al., 2009; Farmer et al., 2010). The critical role of ubiquitination in disease resistance has been demonstrated in many different plant species in the last several years. Identification and characterization of rice (*Oryza sativa*) SPL11, a U-box protein with E3 ligase activity, provided the first direct evidence that ubiquitination controls resistance and programmed cell death (PCD) in plants (Zeng et al., 2004). The *spl11* mutation is characterized by spontaneous cell death in leaves and enhanced disease resistance to bacterial and fungal pathogens in rice (Yin et al., 2000; Zeng et al., 2004). Thus, SPL11 serves as a negative regulator of PCD and defense in rice. In tomato (*Solanum lycopersicum*), a set of E3 ligase genes such as *CMPG1* and *ACRE276*, which are rapidly induced in Avr9-treated Cf-9 tobacco (*Nicotiana tabacum*) cell cultures, were identified as positive regulators of the hypersensitive response (González-Lamothe

[1] This work was supported by the U.S. Department of Agriculture-Cooperative State Research, Education, and Extension Service (grant no. 2007–01667), the National Science Foundation-Integrative Organismal Systems (grant no. 1120949), the U.S. Agency for International Development-International Rice Research Institute Linkage Program (to G.L.W.), by the Natural Science Foundation of China (grant nos. 30871335 to L.D. and 31030047 to Q.X.), and by the Ministry of Science and Technology (grant no. 2011CB915402 to Q.X.).

[2] These authors contributed equally to the article.

[3] These authors contributed equally to the article.

* Corresponding author; e-mail wang.620@osu.edu.

The author responsible for distribution of materials integral to the findings presented in this article in accordance with the policy described in the Instructions for Authors (www.plantphysiol.org) is: Guo-Liang Wang (wang.620@osu.edu).

[C] Some figures in this article are displayed in color online but in black and white in the print edition.

[W] The online version of this article contains Web-only data.

[OA] Open Access articles can be viewed online without a subscription.

www.plantphysiol.org/cgi/doi/10.1104/pp.111.192617

et al., 2006; Yang et al., 2006; van den Burg et al., 2008). In addition, knocking out of *Plant U-box protein17* (*PUB17*), an Arabidopsis (*Arabidopsis thaliana*) ortholog of *ACRE276*, causes compromised RPM1- and RPS4-mediated resistance against *Pseudomonas syringae* pv *tomato* containing the avirulence genes *AvrB* and *AvrRPS4*, respectively (Yang et al., 2006). Similarly, silencing of the F-box gene *ACIF1* compromises the hypersensitive response triggered by various elicitors and by the activation of different *R* genes in tobacco plants (van den Burg et al., 2008).

Flowering is a well-defined plant development process that involves transition from vegetative maturity to the reproductive stage. Multiple external and internal signals, including photoperiod, temperature, hormone, and age-related signals, have been shown to regulate plant flowering. These signals ultimately converge at the floral pathway integrators, a group of genes that are turned on or off to determine the flowering time. Among these flowering pathway integrators, FT and SUPPRESSOR OF OVEREXPRESSION OF CONSTANS1 (SOC1) have been well characterized (Kardailsky et al., 1999; Borner et al., 2000). SOC1 is regulated by two antagonistic flowering regulators, FLOWERING LOCUS C (FLC) and CO, which act as a floral repressor and a floral activator, respectively. CO protein is unstable in the morning and in the dark under long-day (LD) conditions, but the treatment with proteasome inhibitors stabilizes CO, suggesting that CO is targeted for degradation via the 26S proteasome (Valverde et al., 2004). Furthermore, an E3 ligase responsible for the degradation of CO in the dark was identified as the photomorphogenesis-related RING finger protein COP1 (Liu et al., 2008). The light receptor PhyB was shown to be responsible for CO protein instability in the morning, while the blue light receptor CRY2 contributes to the stabilization of CO in the evening and in the dark (Valverde et al., 2004; Liu et al., 2008). CRY2 is ubiquitinated in response to blue light and that ubiquitinated CRY2 is degraded by the 26S proteasome in the nucleus, where it acts as a blue light receptor to promote flowering under LD conditions (Yu et al., 2007). Taken together, these studies suggest that ubiquitination plays a pivotal role in flowering time regulation in Arabidopsis.

The rice *spl11* mutant displays late flowering under LD conditions (Vega-Sánchez et al., 2008). Genetic and molecular analyses showed that SPL11 regulates flowering via interaction with SPL11-interacting protein1 (SPIN1), a member of the STAR family. SPIN1 inhibits flowering by suppressing Hd3a (an ortholog of FT) via Hd1 (an ortholog of CO)-dependent mechanisms under short-day (SD) conditions and by targeting Hd1-independent factors in LD conditions, suggesting that rice SPL11 regulates flowering time probably through ubiquitination of SPIN1, a component associated with rice flowering signaling. However, how SPL11 regulates both defense responses and flowering time in rice is unclear.

Salicylic acid (SA) plays a critical role in plant disease resistance. In addition, SA also regulates plant development (Martínez et al., 2004; Wada et al., 2010). Recently, WIN3 was found to regulate both plant innate immunity and flowering time in Arabidopsis (Wang et al., 2011). WIN3 is a type II SA regulator belonging to the firefly luciferase family that consists of 19 members (Staswick et al., 2005). It plays multiple roles, including conferring broad-spectrum disease resistance to biotrophic and necrotrophic pathogens, modulating cell death in the SA signaling mutant *acd6-1*, and contributing to flg22-induced pathogen-associated molecular pattern (PAMP)-triggered immunity (PTI; Wang et al., 2011). Additionally, WIN3 negatively regulates flowering time under LD conditions via the regulation of FLC and FT (Wang et al., 2011). These data indicate that signaling in the control of plant defense and plant flowering time is interconnected at WIN3.

In this study, we show that the U-box-type E3 ubiquitin ligase PUB13, the ortholog of rice SPL11 in Arabidopsis, regulates cell death, broad-spectrum disease resistance to various pathogens, and flowering time. Our data indicate that PUB13 negatively regulates SA-mediated defense and flowering time in a SID2- and PAD4-dependent manner, which implies that PUB13 plays dual roles in the regulation of both plant defense and development via SA-mediated signaling.

RESULTS

PUB13, Encoding a U-Box/ARM Protein, Is the Closest Arabidopsis Ortholog of Rice SPL11

To identify the putative orthologous gene of *Spl11* in Arabidopsis, we performed BLAST searches against Arabidopsis genome sequences using the amino acid sequence of SPL11 as a query. The data mining identified Arabidopsis PUB13 (At3g46510) as the closet ortholog of SPL11 (Azevedo et al., 2001; Zeng et al., 2008). The protein sequence of PUB13 is highly similar to SPL11, sharing 73% identity of amino acids. The PUB13 protein contains a conserved U-box domain spanning amino acid residues 256 to 329, which is highly similar to that in SPL11 (Fig. 1A; Supplemental Fig. S1A). The highly conserved amino acid residues Val-273, Cys-297, and Pro-298 in known U-box proteins are present in both PUB13 and SPL11. Like SPL11, PUB13 contains six tandem repeats of Armadillo (ARM) motifs in its central region and C terminus, and the *PUB13* gene possesses a similar gene structure to *Spl11* (Fig. 1B). Because of the existence of the ARM repeat domain, PUB13 is classified into PUB family class II (Azevedo et al., 2001). Two other members of the same class, PUB14 and PUB17, have been implicated in cell death and disease resistance, respectively (Yang et al., 2006; Yee and Goring, 2009).

PUB13 Possesses E3 Ligase Activity in Vitro, and the U-Box Domain Is Required for E3 Ligase Activity

Possession of E3 ubiquitin ligase activity is an important feature of U-box-containing proteins (Hatakeyama et al., 2001; Mudgil et al., 2004). To analyze E3 ubiquitin

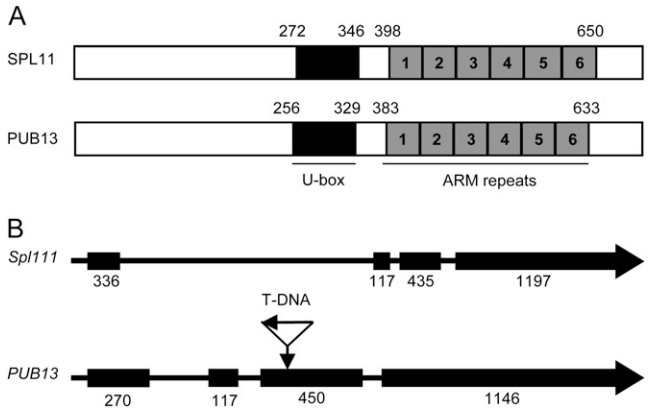

Figure 1. The protein and gene structures between PUB13 and SPL11. A, Schematic representation of PUB13 and SPL11 proteins. The black box indicates the U-box domain, and the individual ARM repeats are indicated by numbered gray boxes. Numbers above the schematic representation indicate the positions of amino acid residues. B, Gene structures of *PUB13* and *Spl11*. Exons are represented as black boxes. The number below each exon indicates the length of the exon in bp. The position of the T-DNA insertion in the *pub13* mutant is marked by an arrow.

ligase activity of PUB13 in vitro, we fused the full-length cDNA of the *PUB13* gene to glutathione *S*-transferase (GST) and expressed it in *Escherichia coli*. In the E3 ligase activity assay, the purified GST-PUB13 was incubated in the presence or absence of wheat E1 (GI: 136632), human E2 UBCH5b, and/or His-tagged ubiquitin. Ubiquitination activity was detected by immunoblot with nickel-horseradish peroxidase. In the presence of E1, E2, and ubiquitin, GST-PUB13 showed a strong ligase activity by forming high-molecular-mass polyubiquitin (Fig. 2, lane 4, top panel).

To find out whether an intact U-box domain is necessary for the E3 ligase activity of PUB13, we made the mutant construct GST-PUB13 ($V^{273}R$) by substituting Val-273 to Arg in the U-box domain. This Val is highly conserved in different U-box proteins and was demonstrated to be important for the biological and biochemical functions of U-box proteins (Ohi and Gould, 2002; Zeng et al., 2004). Under the same analysis conditions, GST-PUB13 ($V^{273}R$) showed much reduced ligase activity compared with wild-type PUB13 (Fig. 2Fig. 2, lane 6, top panel). The anti-GST immunoblot was used to confirm the presence of the similar amount of GST-fused proteins in the assay. As shown in Figure 2 (bottom panel), GST-PUB13 fusions were presented in reactions as expected, and self-ubiquitination of GST-PUB13 was also detected in the anti-GST immunoblot in the presence of E1, E2, and ubiquitin (Fig. 2, lane 4, bottom panel). Consistent with the nickel-horseradish peroxidase immunoblot, anti-GST also showed that the self-ubiquitination of PUB13 ($V^{273}R$) was significantly suppressed (Fig. 2, lane 6, bottom panel). These results indicate that PUB13 possesses E3 ligase activity and that the intact U-box domain is required for its activity.

Cell Death and Hydrogen Peroxide Accumulation Are Elevated in *pub13*

We identified a T-DNA insertion mutant, *pub13*, in the Arabidopsis Biological Resource Center mutant collection, in which the T-DNA insertion was located at the third exon of *PUB13* (Fig. 1B). Gene expression analysis showed that the transcription of *PUB13* is completely abolished in *pub13* (Supplemental Fig. S1B). Under LD growth conditions (23°C, 70% relative humidity [RH], 16 h of daylight/8 h of dark), we found that the lower leaves of the *pub13* mutant displayed chlorosis and lesion-mimic phenotypes spontaneously, and the chlorosis was formed from leaf edge to main vein (Fig. 3A). To check whether this lesion-mimic phenotype is associated with cell death, the leaves of *pub13* were subjected to trypan blue

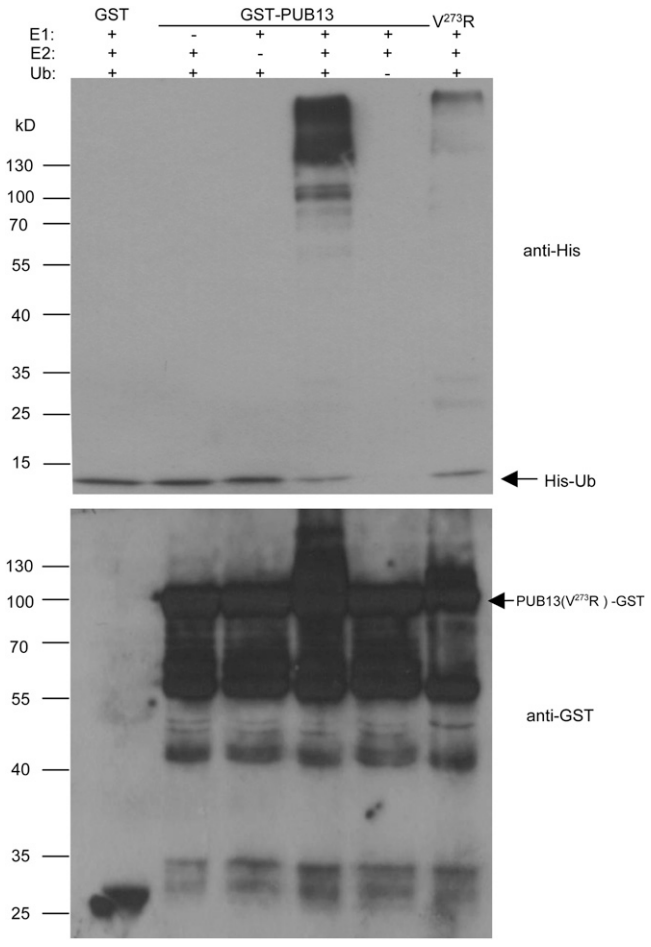

Figure 2. Analysis of E3 ubiquitin ligase activity for PUB13. An in vitro ubiquitination assay was performed with GST-PUB13/$V^{273}R$ fusion proteins in the presence or absence of wheat E1, human E2 (UBCH5b), and His-tagged ubiquitin. The numbers on the left denote the molecular masses of marker proteins in kD. The ubiquitination signal was detected using nickel-horseradish peroxidase (top panel). The expression of GST-fused proteins in the assay was detected with an anti-GST immunoblot (bottom panel).

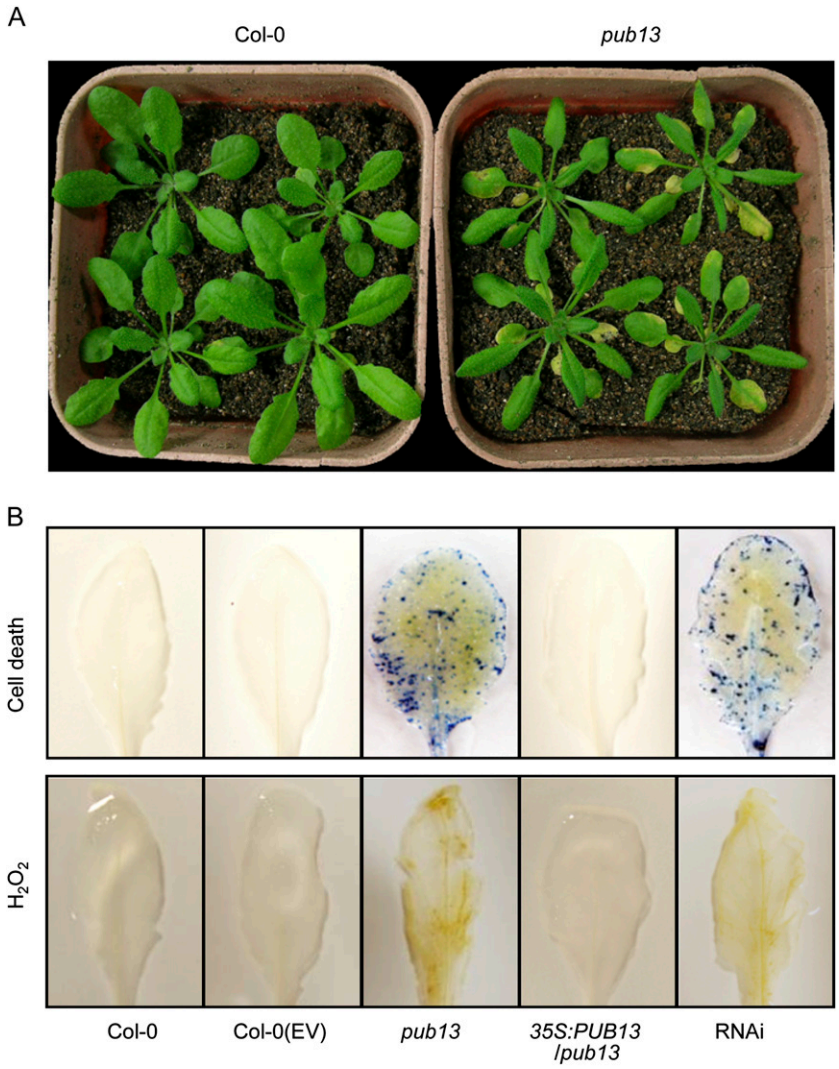

Figure 3. Cell death and H_2O_2 accumulation in *pub13*, complemented *pub13*, and *PUB13* RNAi transgenic plants. A, Lesion-mimic phenotype of *pub13*. Plants were 4 weeks old and grown under LD conditions. B, Cell death and H_2O_2 accumulation in *pub13*, complemented *pub13*, and *PUB13* RNAi transgenic plants. Cell death and H_2O_2 accumulation were examined in the lower leaves of *pub13* with chlorosis and leaves at the same positions of other lines. Plants were 4 weeks old and grown under LD conditions. The leaves in the top panel were stained with trypan blue for cell death. H_2O_2 accumulation was detected by DAB staining in the bottom panel. EV, Empty vector used for the RNAi construct.

staining. The lower leaves of *pub13* with chlorosis were stained blue, whereas the leaves at the same position in wild-type ecotype Columbia (Col-0) were not (Fig. 3B, top panel). In the middle-aged green leaves of *pub13* (i.e. the seventh or eighth leaf of 4-week-old plants), cell death was also detected, although no macroscopic death was visible (Supplemental Fig. S2B, top panel).

To confirm whether the cell death is caused by the knockout of *PUB13*, we transformed the intact *PUB13* coding sequence with 35S promoter into *pub13* and a *PUB13* RNA interference (RNAi) construct into Col-0. Trypan blue staining assays showed that the non-cell-death phenotype was restored in the *PUB13*-complemented *pub13* transgenic plants (Fig. 3B, top panel) while the lower leaves of *PUB13* RNAi lines showed clear cell death like that in *pub13* (Fig. 3B, top panel). These results demonstrate that PUB13 negatively controls cell death in Arabidopsis.

Since reactive oxygen species are key players in the regulation of PCD, we measured the accumulation of hydrogen peroxide (H_2O_2) in *pub13*, complemented *pub13*, and RNAi lines. The lower leaves of these lines grown under LD conditions were stained by 3,3′-diaminobenzidine tetrahydrochloride (DAB). In agreement with the cell death phenotypes, the H_2O_2 content in lower leaves of *pub13* and *PUB13* RNAi lines was markedly increased, but this increase was restored to the wild-type level in complemented *pub13* plants (Fig. 3B, bottom panel). Interestingly, no difference was observed in the H_2O_2 level for the middle-aged leaves of *pub13* and Col-0 (Supplemental Fig. S2B, bottom panel).

The Increase of Cell Death and H_2O_2 Accumulation in *pub13* Depends on the SA Signal

The PCD is closely associated with SA via an unclear mechanism (Ludwig and Tenhaken, 2000; Kawai-Yamada et al., 2004). We introduced the SA induction-deficient mutant *sid2-2* into *pub13* by genetic cross and analyzed the role of SA for cell death increase in *pub13*. Leaves of 4-week-old plants grown under LD and high-humidity

conditions (see details below) were collected for trypan blue staining. As shown in Figure 4A, cell death was suppressed significantly in the *pub13sid2-2* double mutant compared with the clear cell death phenotype in *pub13*, and no visible cell death was observed in *sid2-2* and Col-0. Another SA-deficient mutant, *pad4*, was also introduced into *pub13* to confirm the *pub13sid2-2* result. Similarly, the cell death in the *pub13pad4* double mutant was considerably suppressed under LD and high-humidity conditions (Fig. 4B).

The role of *sid2-2* and *pad4* for the H_2O_2 accumulation in *pub13* was also determined. After high-humidity treatment, the H_2O_2 level in *pub13* increased significantly compared with that of Col-0 but the H_2O_2 content in *sid2-2* was at a similar level to Col-0 (Fig. 4C). Notably, the H_2O_2 accumulation in the *pub13sid2-2* double mutant was reduced to a background level. Similarly, introduction of *pad4* into *pub13* reduced the high H_2O_2 accumulation in *pub13* to the normal level under LD and high-humidity conditions (Fig. 4D). The elimination of cell death and H_2O_2 accumulation in *pub13sid2-2* and *pub13pad4* suggests that SA is required for the spontaneous cell death and elevated H_2O_2 accumulation in *pub13*.

The *pub13* Mutant Confers Enhanced Resistance against Biotrophic Pathogens

The PCD phenotype and H_2O_2 accumulation in *pub13* led us to investigate the function of *PUB13* in plant defense. We first inoculated the Col-0 and *pub13* plants grown under LD conditions with the virulent strain ES4326 of the biotrophic pathogen *Pseudomonas syringae* pv *maculicola* (*Psm*). Three days after inoculation, the water-soaked lesions of *pub13* leaves were smaller than those in Col-0 leaves (Fig. 5A, left panel). To monitor the growth of bacteria, *Psm* ES4326 was infiltrated into *pub13* and Col-0 plants at a low titer. The bacterial growth analysis showed that the amount of bacteria in Col-0 was more than that in *pub13* (Fig. 5A, right panel), suggesting that the *pub13* mutation confers elevated resistance to the biotrophic bacterial pathogen *Psm* ES4326.

To test whether *pub13* confers elevated resistance to biotrophic fungal pathogens as well, we inoculated both *pub13* and Col-0 with *Erysiphe cichoracearum* UCSC1, which causes powdery mildew diseases in many plants. Abundant conidiophores and conidiophore peduncles spread all over the Col-0 leaves but much less on the *pub13* leaves, and visible cell death appeared in the infected *pub13* leaves at 7 d post inoculation (dpi; Fig. 5B, left panel). To further confirm the resistance of *pub13* to UCSC1, we stained the inoculated Col-0 and *pub13* leaves with trypan blue at 10 dpi. As shown in Figure 5B (right panel), a large number of hyphae and conidiophores existed in Col-0 while only a few hyphae were observed in *pub13*. These results indicate that *pub13* confers enhanced resistance to the biotrophic fungus strain UCSC1.

In addition to examining the resistance of *pub13* against biotrophic pathogens, we also tested whether *pub13* confers resistance to the necrotrophic fungal pathogens *Botrytis cinerea* BO5-10 and *Alternaria brassicicola* AB. In contrast to biotrophic pathogens, no significant difference in disease symptom and pathogen growth was observed when the mutant and wild-type plants were inoculated with these two fungal pathogens under LD and normal-humidity conditions (70% RH; Supplemental Fig. S3, C and D).

Cell Death, H_2O_2 Content, and Disease Resistance of *pub13* Are Increased under High Humidity

It is known that some lesion-mimic mutants are sensitive to environmental stress conditions such as high humidity (Mosher et al., 2010). To test the effect of humidity on the occurrence of the phenotypes on *pub13* plants, 4-week-old *pub13* plants grown under regular conditions (approximately 70% RH) were subjected to high-humidity (95% RH) treatment. After 48 h of high-humidity treatment, the lesion-mimic phenotype of *pub13* was more severe than that in wild-type plants (Supplemental Fig. S2A). Consistent with the lesion-mimic phenotype, cell death in middle-aged leaves of *pub13* after high-humidity treatment was much stronger compared with that in untreated plants (Supplemental

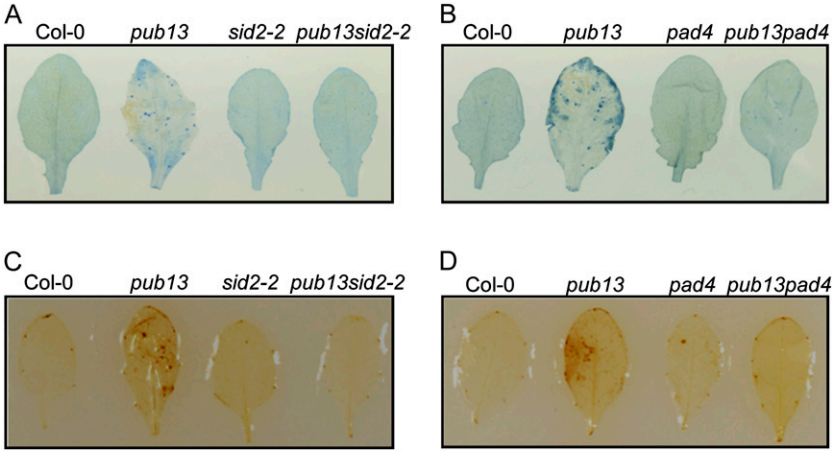

Figure 4. Cell death and H_2O_2 accumulation in the *pub13sid2-2* and *pub13pad4* mutants. Four-week-old plants grown under LD conditions were treated with high humidity (95% RH) for 48 h, and then cell death and H_2O_2 accumulation were detected in the middle-aged leaves (i.e. the seventh or eighth leaves in 4-week-old plants). A, Cell death in Col-0, *pub13*, *sid2-2*, and *pub13sid2-2*. B, Cell death in Col-0, *pub13*, *pad4*, and *pub13pad4*. C, H_2O_2 accumulation in Col-0, *pub13*, *sid2-2*, and *pub13sid2-2*. D, H_2O_2 accumulation in Col-0, *pub13*, *pad4*, and *pub13pad4*.

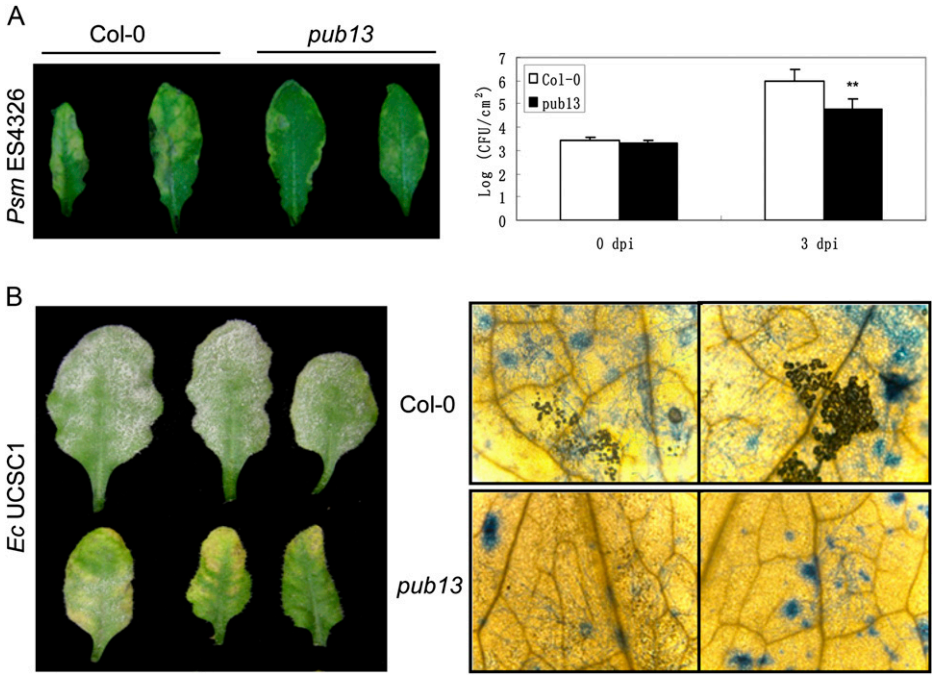

Figure 5. Disease resistance of *pub13* against biotrophic pathogens. A, Disease symptoms and bacterial growth assays of *Psm* ES4326 in Col-0 and *pub13* under LD conditions. Disease symptoms (left panel) were photographed on day 3 after spraying with 1×10^8 CFU mL^{-1} ES4326. Bacterial growth (right panel) was assessed in the leaves injected with 1×10^5 CFU mL^{-1} ES4326. Student's *t* test was carried out to determine the significance of the difference between Col-0 and *pub13* plants. ** Significant difference at $P < 0.01$. B, Phenotypes of Col-0 and *pub13* grown under LD conditions against *E. cichoracearum* (*Ec*) UCSC1. Plants were inoculated with conidia (approximately 100 conidia mm^{-2}) of UCSC1. Inoculated plants were photographed at 7 dpi (left panel) or photographed using a microscope after staining with trypan blue at 10 dpi (right panel). These experiments were repeated at least twice with similar results.

Fig. S2B, top panel). In addition, the middle-aged leaves from humidity-treated *pub13* but not from treated Col-0 exhibited abundant H_2O_2 accumulation, while there was no obvious H_2O_2 accumulation in the middle-aged leaves of untreated *pub13* (Supplemental Fig. S2B, bottom panel). Humidity, therefore, can enhance cell death and H_2O_2 accumulation in *pub13* plants.

To test whether the enhanced cell death and H_2O_2 accumulation in *pub13* is correlated with its elevated resistance to pathogen infections, we monitored the level of resistance of *pub13* and Col-0 plants pretreated with high humidity for 24 h. Treated and untreated plants were inoculated with the biotrophic pathogens *P. syringae* pv *tomato* DC3000 and *Hyaloperonospora parasitica* Noco2. Under regular humidity, the disease symptoms of *pub13* inoculated with *P. syringae* pv *tomato* DC3000 (1×10^8 colony-forming units [CFU] mL^{-1}) were milder than those of Col-0 at 5 dpi (Supplemental Fig. S3A, top panel). Analysis of bacterial growth also showed that *pub13* plants were more resistant against DC3000 than Col-0 (Supplemental Fig. S3A, bottom panel). Interestingly, a much larger difference of resistance against DC3000 was observed between the high-humidity-pretreated *pub13* and Col-0 (Supplemental Fig. S3A). High-humidity-pretreated leaves of Col-0 displayed an atrophic and chlorosis phenotype, whereas only some local chlorosis existed on *pub13* leaves. Similar to the inoculation with DC3000, *pub13* was slightly more resistant than Col-0 to Noco2 without humidity treatment (Supplemental Fig. S3B). After pretreatment of high humidity, however, the resistance of *pub13* was much increased, as revealed by less chlorosis symptoms and smaller lesions on the leaves (Supplemental Fig. S3B).

The resistance of *pub13* against the necrotrophic pathogens *B. cinerea* and *A. brassicicola* after high-humidity treatment was also examined. The detached leaves of *pub13* and Col-0 did not show any difference in lesion size under regular humidity after inoculation with *B. cinerea* BO5-1 (Supplemental Fig. S3C). Nevertheless, after high-humidity treatment, leaves of *pub13* plants displayed severe rotting symptoms and large lesions, while no visible necrotic lesion occurred in leaves of Col-0 plants (Supplemental Fig. S3C). Similar to challenge by *B. cinerea*, there was no visible symptom difference from *A. brassicicola* AB between *pub13* and Col-0 under normal humidity (Supplemental Fig. S3D). Conversely, *pub13* was much more susceptible to *A. brassicicola* AB than Col-0 when the plants were pretreated with high humidity (Supplemental Fig. S3D), corroborating the observation that high humidity promotes the susceptibility of *pub13* against necrotrophic pathogens.

PAD4 and SID2 Are Required for the PUB13-Mediated Resistance to *Psm* ES4326 But Not to *B. cinerea* BO5-10

As mentioned above, the cell death and H_2O_2 accumulation in *pub13* are dependent on the SA signaling components SID2 and PAD4. To test the function of *SID2* and *PAD4* genes in the *PUB13*-mediated defense pathway, we inoculated the *pub13sid2-2* and *pub13pad4* plants with the biotrophic pathogen ES4326. Under regular-humidity and LD conditions, *pub13* displayed elevated resistance but *sid2-2* showed reduced resistance against ES4326 (Fig. 6A). As expected, the resistance of the *pub13sid2-2* double mutant against ES4326 was markedly reduced to a level even more susceptible than Col-0. Similarly, the *pub13pad4* plants were slightly more susceptible than Col-0 (Fig. 6B). In contrast to the biotrophic pathogens, the resistance level of *pub13sid2-2* and *pub13pad4* plants against the necrotrophic pathogen BO5-10 was comparable to that of *pub13* plants after high-humidity treatment (Fig. 6C). Taken together, these results demonstrated that SID2 and PAD4 are required for *PUB13*-mediated resistance to the biotrophic pathogen ES4326 but are dispensable for resistance to the necrotrophic pathogen BO5-10.

The *pub13* Mutant Contains Elevated Levels of SA

The intimate involvement of *PUB13* in host defense against biotrophic and necrotrophic pathogens prompted us to determine the expression levels of known defense-related genes in *pub13*. The transcriptional levels of *PR1*, a marker gene in the SA signaling pathway, and *PDF1.2*, a marker gene of the jasmonic acid (JA) and ethylene (ET) signaling pathways, were examined in Col-0 and *pub13* plants grown under LD conditions using real-time PCR. As shown in Supplemental Figure S4A, the transcriptional level of *PR1* was significantly induced in *pub13* compared with Col-0, whereas *PDF1.2* was markedly suppressed in *pub13*. We then determined the SA levels in Col-0 and *pub13* plants by HPLC. Total SA was extracted from 0.2 g (fresh weight) of leaves of 4-week-old Col-0 and *pub13* plants grown under LD conditions. As expected, the SA content in *pub13* was 63% higher than in Col-0 (Supplemental Fig. S4B). Although the SA level was undetectable in both SA signal deficiency mutants *sid2-2* and *pad4*, the increased SA level in *pub13* was greatly reduced in the *pub13sid2-2* and *pub13pad4* double mutant plants, only 10% and 32% of that of Col-0, respectively (Supplemental Fig. S4B), suggesting that PUB13 negatively regulates SA accumulation via both SID2 and PAD4.

PUB13 Is a Negative Regulator of Flowering Time

During the reproductive development stage of the *pub13* mutant, we found that the mutant displayed altered flowering time. We grew the *pub13* plants under different photoperiod conditions: SD (8 h of daylight/16 h of dark), MD (for middle day; 12 h of daylight/12 h of dark), and LD (16 h of daylight/8 h of dark). Under

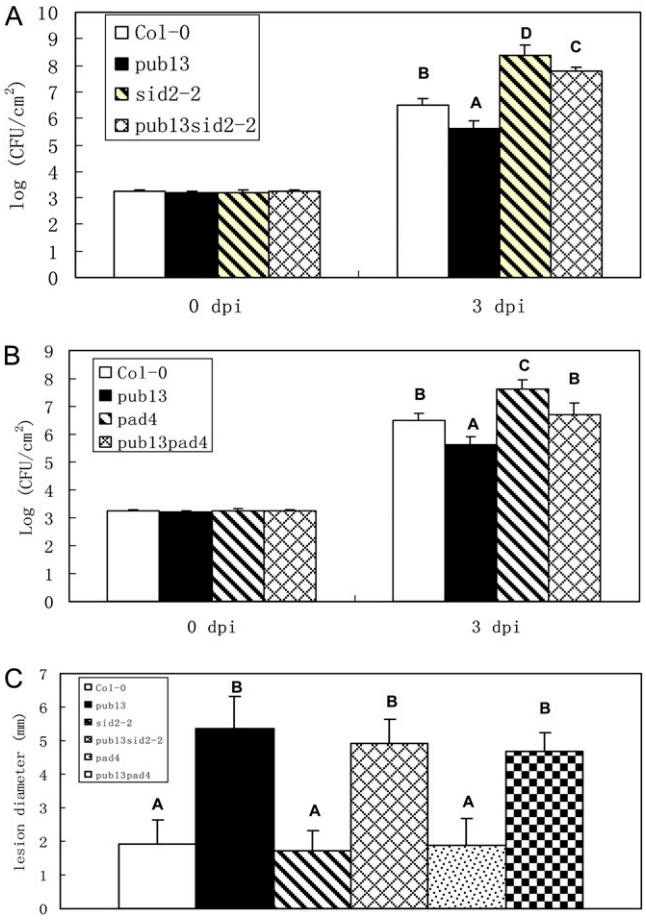

Figure 6. Disease reaction of the *pub13sid2-2* and *pub13pad4* double mutants against *Psm* ES4326 and *B. cinerea* BO5-10. A, Resistance of *pub13sid2-2* against ES4326. B, Resistance of *pub13-pad4* to ES4326. Four-week-old plants in A and B were grown under LD conditions and injected with 1×10^5 CFU mL^{-1} ES4326. C, Resistance of *pub13sid2-2* and *pub13pad4* double mutants to BO5-10. Detached leaves from high-humidity-pretreated plants grown under LD conditions were inoculated with 5 μL of conidia suspension (1×10^4 conidia mL^{-1}) of BO5-10, and lesion diameter was measured at 3 dpi. All the experiments were repeated at least twice with similar results. Student's *t* test was carried out to determine the significance of the difference. Uppercase letters indicate significant difference at $P < 0.01$. [See online article for color version of this figure.]

SD conditions, there was no significant difference between Col-0 and *pub13* in flowering time, except that a few *pub13* plants exhibited slightly earlier flowering than Col-0 (Fig. 7A, left panel). However, under LD conditions, *pub13* flowered about 4 d earlier than Col-0 (Fig. 7A, right panel). The early-flowering phenotype of *pub13* under MD conditions was even more significant compared with Col-0 (Fig. 7A, middle panel). The leaf number of *pub13* before flowering was four and six less than Col-0 under LD and MD conditions, respectively, while the leaf number of *pub13* was slightly less than Col-0 under SD conditions (Fig. 7B). Under LD conditions,

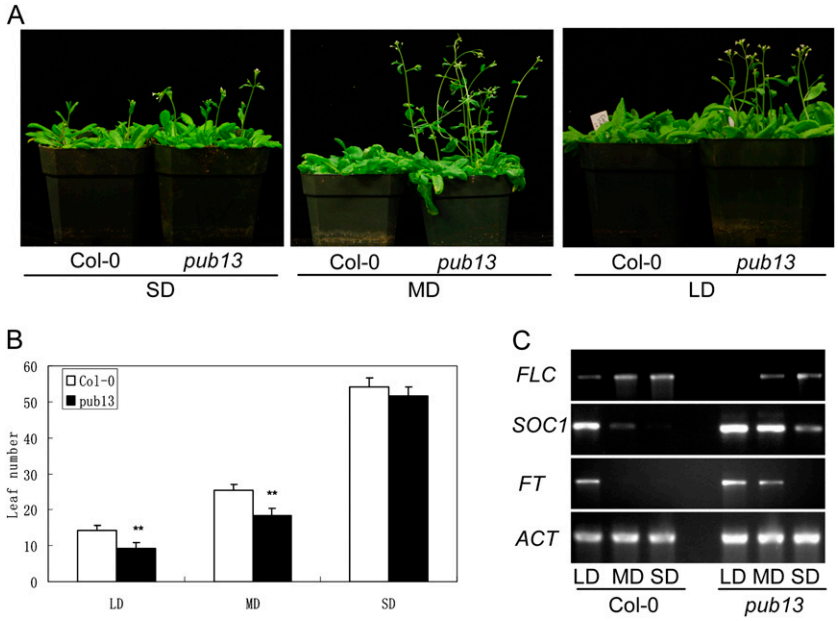

Figure 7. Flowering phenotypes and RT-PCR analysis of flowering marker genes in *pub13*. A, Flowering phenotypes of Col-0 and *pub13* grown under SD, MD, and LD conditions. B, Leaf number of Col-0 and *pub13* under SD, MD, and LD conditions. The leaf number was counted when the first flower bud appeared. Statistical analysis was carried out as for Figure 5. C, Expression of flowering marker genes in Col-0 and *pub13* under SD, MD, and LD conditions. Gene expression of *FLC*, *SOC1*, and *FT* in Col-0 and *pub13* was determined by RT-PCR. *Actin* (*ACT*) was used as a control for loading.

the *PUB13* RNAi plants also exhibited early flowering; however, the early-flowering phenotype was abolished in the complemented *pub13* plants (Supplemental Fig. S5). These results indicate that PUB13 acts as a suppressor of flowering time.

To understand how PUB13 regulates the floral transition, we analyzed the transcript levels of the floral repressor *FLC* and the floral activators *FT* and *SOC1* in *pub13* under SD, MD, and LD conditions. As shown in Figure 7C, the transcript level of *FLC* in Col-0 was higher than in *pub13* under LD and MD conditions, and there was no visible difference under SD conditions. On the contrary, the transcriptional level of *SOC1* in Col-0 was lower than in *pub13* under LD, MD, and SD conditions. Similarly, the transcript level of *FT* in Col-0 was also lower than in *pub13* under LD and especially under MD conditions. Taken together, these data suggested that PUB13 regulates flowering time probably through the SOC1-mediated flowering pathway.

PUB13 Regulates Flowering Time Mainly through a SA-Dependent Pathway

SA is not only a critical regulator of plant defense but also is involved in the regulation of plant flowering time (Martínez et al., 2004). Thus, we investigated the relationship between PUB13-mediated flowering time and the SA pathway. To this purpose, the flowering time of *pub13sid2-2* and *pub13pad4* was examined under LD conditions. As shown in Figure 8A, the early flowering observed in *pub13* was suppressed in both *pub13sid2-2* and *pub13pad4*, while the flowering time of *sid2-2* and *pad4* single mutants was the same as in Col-0. The leaf number of *pub13sid2-2* and *pub13pad4* before the appearance of the first floral bud was almost the same as in Col-0, which was four to five leaves more than *pub13* (Fig. 8B). Analysis of the expression level of flowering marker genes in these plants under LD conditions revealed that the expression of *FLC* was suppressed in *pub13* but was restored in *pub13sid2-2* and *pub13pad4*, and the expression level of *FLC* in *sid2-2* and *pad4* was comparable to that in Col-0 (Fig. 8C). On the contrary, the transcript levels of *SOC1* and *FT* were increased in *pub13* but were similar in *pad4*, *sid2-2*, and Col-0. However, the expression levels of *SOC1* and *FT* were reduced in *pub13sid2-2* and *pub13pad4* compared with those in *pub13* (Fig. 8C). These results suggest that PUB13 regulates flowering time in a SA signaling-dependent manner.

DISCUSSION

The ubiquitin proteasome system (UPS)-mediated protein modification and degradation has been recognized as a critical mechanism in the regulation of numerous cellular processes in plants. The importance of the UPS in plant innate immunity and flowering has been well documented in plants (Henriques et al., 2009; Trujillo and Shirasu, 2010). Many UPS-related components have been implicated in either of the two biological processes. Nevertheless, the interconnection between the signaling pathways underlying these two processes via the UPS has not yet been reported. In this study, we extensively analyzed the functions of the Arabidopsis *PUB13* gene in both innate immunity and flowering. We found that *PUB13* encodes a U-box/ARM repeat protein endowed with E3 ligase activity. Genetic and physiological analysis revealed that PUB13 negatively regulates cell death, H_2O_2 accumulation, and defense against biotrophs but positively regulates the

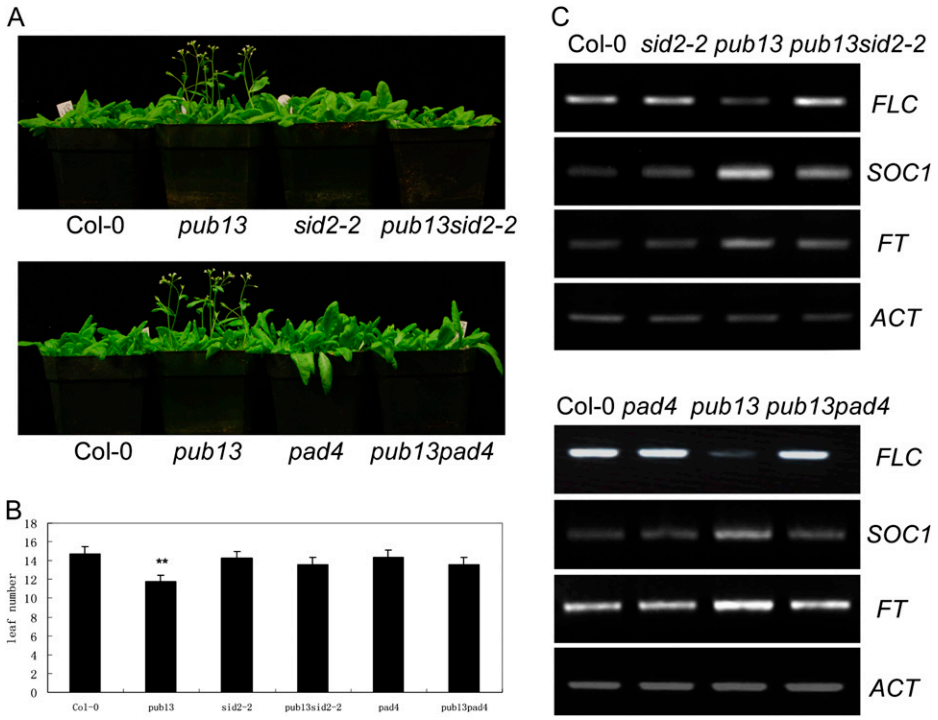

Figure 8. Flowering phenotypes and expression of flowering marker genes in the *pub13sid2-2* and *pub13pad4* double mutants. A, Flowering phenotypes of *pub13*, *pub13sid2-2*, and *pub13pad4* grown under LD conditions. B, Leaf number of Col-0, *pub13*, *sid2-2*, *pub13-sid2-2*, *pad4*, and *pub13pad4* grown under LD conditions. Leaf number for each genotype was counted once the first flower bud appeared. Statistical analysis was carried out as for Figure 5. C, Flowering marker gene transcription levels. Gene expression of *FLC*, *SOC1*, and *FT* in 4-week-old plants grown under LD conditions was detected with RT-PCR. *Actin* (*ACT*) was used as a loading control.

resistance to necrotrophic pathogens. We discovered that PUB13 is a negative regulator of flowering time under MD and LD conditions and that the PUB13-mediated regulation of flowering time is probably through the SOC1-mediated signaling pathway. Our results revealed dual roles for PUB13 and provided novel evidence that innate immunity and development are interconnected via the UPS in Arabidopsis.

SA is a critical signaling molecule in the pathways of local and systemic resistance in plants. In *pub13*, the elevated SA level is associated with enhanced defense responses. After suppressing SA in *pub13* through the introduction of *sid2-2* or *pad4*, the enhanced defense responses of *pub13* are largely repressed. Therefore, PUB13 regulates plant defense responses through a SA-dependent pathway. Stresses usually can promote plant early flowering and SA accumulation (Wada and Takeno, 2010; Wada et al., 2010). Previous research showed that SA is a positive regulator of flowering not only in stressed plants but also in nonstressed plants (Martínez et al., 2004). We found that the SA level, cell death, and H_2O_2 accumulation, which are usually altered as responses to stress, are elevated in *pub13* in a nonstressed environment, suggesting that these responses in *pub13* trigger early flowering, perhaps by mimicking stress signaling.

Genetic and biochemical analyses indicated that early flowering is suppressed when the SA level in *pub13* is reduced by knocking out *SID2* or *PAD4*. Thus, the genes involved in SA-mediated defense signaling, *PUB13*, *SID2*, and *PAD4*, are also involved in floral transition control, which suggests that plant innate immunity and development are intimately linked at SA-mediated signaling. However, it is still unclear how PUB13 regulates flowering through the SID2/PAD4-mediated SA signaling pathway. A previous study suggested that SA regulates flowering time probably through the photoperiod and vernalization flowering pathways that are independent on FLC, CO, and FCA (Martínez et al., 2004). Consistent with this notion, we found in this study that the transcript levels of the flowering marker genes *FLC*, *SOC1*, and *FT* remain unchanged in *sid2-2* and *pad4* single mutants. Therefore, further study is needed to find out whether PUB13-SID2/PAD4 also function in other flowering pathways and how the corresponding flowering pathway interconnects with plant innate immunity through PUB13-SID2/PAD4.

Numerous studies have shown that effective plant resistance to biotrophs is largely dependent on PCD and the activation of defense responses regulated by the SA pathway. On the contrary, necrotrophs benefit from the cell death of host plants, and the host defense responses are mainly modulated by the JA/ET pathways. We found that the *pub13* mutant contains elevated levels of SA and confers enhanced resistance against four biotrophs (*Psm* ES4326, *E. cichoracearum* UCSC1, *P. syringae* pv *tomato* DC3000, and *H. parasitica* Noco2). When the SA levels are reduced in *pub13* through introducing *sid2-2* or *pad4*, elevated disease resistance to the biotrophs is abolished, indicating that SA signaling is indispensable for PUB13-regulated resistance to biotrophs. Conceivably, due to antagonism between SA and JA/ET, the JA/ET signal and *PDF1.2* expression are suppressed in *pub13*, which displays susceptibility to two necrotrophs (*B. cinerea*

BO5-10 and *A. brassicicola* AB) under high-humidity conditions.

A role of PUB proteins in PTI has been reported in recent years. For example, a homologous triplet of PUB proteins, PUB22, PUB23, and PUB24, in Arabidopsis negatively regulates PTI in response to multiple PAMPs (Trujillo et al., 2008). A more recent study also showed that PUB13 is involved in preventing prolonged/excessive activation of FLS2-mediated PTI (Lu et al., 2011). PUB13 and its close homolog PUB12 were found to polyubiquitinate their substrate FLS2, a pattern-recognition receptor of bacterial flagellin. PUB13 and PUB12 promote FLS2 degradation after the cells are stimulated by flg22, a 22-amino acid peptide derived from the conserved region of bacterial flagellin (Lu et al., 2011). The receptor-like kinase BAK1, which forms a receptor complex with FLS2 immediately upon flagellin stimulation, can phosphorylate both PUB13 and PUB12, and this phosphorylation is required for the flagellin-induced FLS2-PUB13/PUB12 association (Chinchilla et al., 2007; Lu et al., 2011). Furthermore, flagellin-induced transient reactive oxygen species burst is increased in the *pub12* and *pub13* single mutants compared with the wild type, although FLS2 is not constitutively accumulated in *pub12/pub13* (Lu et al., 2011). To further confirm the function of PUB13 in PAMP signaling, we examined pretreated flg22-induced resistance in *pub13* against subsequent infection of the virulent strain DC3000. The flg22-induced resistance in *pub13* is not significantly different compared with the wild type (data not shown), probably due to functional redundancy between PUB13 and PUB12. Since PUB13 ubiquitinates FLS2 and plays a negative role in FLS2 signaling, we also investigated whether FLS2 functions in flowering. We planted *fls2* mutant and *FLS2* transgenic lines in the Col-0 background under MD and LD conditions, respectively, and found that the flowering phenotypes of *fls2* and FLS2 transgenic plants are the same as in the wild type (data not shown), suggesting that FLS2 does not relate to flowering.

Sequence and gene structure analyses revealed that *PUB13* is the putative ortholog of the rice E3 ligase gene *SPL11*. SPL11 was found to negatively regulate cell death and defense but to positively regulate flowering time under LD conditions, probably through ubiquitination of SPIN1 in rice (Zeng et al., 2004; Vega-Sánchez et al., 2008). In this study, we report that PUB13 regulates cell death, defense, as well as flowering time through a SA-dependent pathway. Although PUB13 plays a similar role to SPL11 in defense, it acts as a negative regulator of flowering time in Arabidopsis under LD and MD conditions. This difference is due to the fact that Arabidopsis is a LD plant and rice is a SD plant. Interestingly, our genetic complementation showed that the early-flowering and cell death phenotypes of *pub13* were restored when the rice *Spl11* gene was expressed in the *pub13* plants under the control of the 35S promoter (Supplemental Fig. S6), indicating that the functions of PUB13/SPL11 are highly conserved in dicot and monocot plants. Further characterization of PUB13/SPL11 and other associated components, therefore, should provide exciting insights into the interconnection and coordination of innate immunity and development in plants.

MATERIALS AND METHODS

Plants, Growth Conditions, and High-Humidity Treatment

Arabidopsis (*Arabidopsis thaliana*) wild-type (Col-0), *pub13* (Salk_093164), *sid2-2* (Wildermuth et al., 2001), *pad4* (Glazebrook et al., 1996), and *fls2* (Xiang et al., 2008) were used in this study. *pub13* was obtained from the Arabidopsis Biological Resource Center and confirmed with PCR primers: PUB13-1F (5′-ATGGAGGAAGAGAAAGCTTC-3′), LBb1 (5′-GCGTGGACCGCTTGCTGCAACT-3′), and PUB13-1074R (5′-CATAAGATCTTCAATCTTGTTCGC-3′). *pub13sid2-2* and *pub13pad4* were made by genetic crosses. To generate *PUB13*-complemented *pub13* (35S:*PUB13*/*pub13*), the full-length cDNA of *PUB13* was amplified from Col-0 cDNA and cloned into pEarleyGate 101. Then, the *Agrobacterium tumefaciens*-mediated flower-dipping method of transformation was performed according to a standard protocol to get 35S:*PUB13*/*pub13* transgenic plants. To generate *PUB13* RNAi plants, an artificial microRNA targeting *PUB13* was cloned into the binary vector pKANNIBAL as described previously (Schwab et al., 2006), and the new construct was transformed into Col-0. FLS2 transgenic plants were made as described (Xiang et al., 2008). Plants were grown under 22°C, 70% RH, and light intensity of 250 μmol photons m^{-2} s^{-1} with 8 h of daylight/16 h of dark as SD, 12 h of daylight/12 h of dark as MD, or 16 h of daylight/8 h of dark as LD. For high-humidity treatment, plants were transferred to a dew chamber and a humidifier was used to keep the humidity about 95% RH.

Trypan Blue and DAB Staining

Trypan blue staining was performed for cell death assay as described previously (Bowling et al., 1994). To determine the accumulation of H_2O_2, we stained the selected leaves with DAB as described previously (Wohlgemuth et al., 2002). Briefly, leaves were stained with 0.1% (w/v) DAB for 8 h in the dark, destained with 95% ethanol, and preserved in 50% ethanol. The leaves for trypan blue or DAB staining were pretreated with high humidity for 48 h.

Pathogen Inoculation

Four-week-old plants grown under LD conditions were inoculated with different pathogens. To detect the humidity effect on disease resistance, the plants were treated with high humidity (95% RH) for 24 h, and then the treated plants or detached leaves were used for inoculation with different pathogens. *Pseudomonas syringae* pv *maculicola* ES4326 and *Pseudomonas syringae* pv *tomato* DC3000 were sprayed on the plants with 1×10^8 CFU mL^{-1} for disease symptoms or injected with 5×10^5 CFU mL^{-1} for bacterial growth assay. The flg22 protection analysis was performed as described previously (Zhang et al., 2010). *Erysiphe cichoracearum* UCSC1 was inoculated as described (Vorwerk et al., 2007), and the macroscopic symptoms were observed at 7 dpi and the microscopic symptoms were checked at 10 dpi after trypan blue staining. For *Botrytis cinerea* inoculation, the fungus was cultured on a potato dextrose agar plate for 2 weeks at 24°C with a 12-h photoperiod. The fungal culture was washed with water and filtered with a nylon mesh. Then, the conidia were resuspended in potato dextrose broth and the concentration was adjusted to 1×10^4 conidia mL^{-1}. The detached rosette leaves were placed in petri dishes containing 0.8% agar, and 5 μL of conidia suspension was dropped on the leaf surface. The petri dishes with the inoculated leaves were incubated at 22°C with a 12-h photoperiod. The diameter of the lesion was measured at 3 dpi. Inoculation of detached leaves with *Alternaria brassicicola* (1×10^5 spores mL^{-1}) was performed as described previously (van Wees et al., 2003). Photographs were taken and lesion diameter was measured at 3 dpi. For the inoculation of *Hyaloperonospora parasitica* Noco2, plants were sprayed with 1×10^5 spores mL^{-1}, then the inoculated plants were kept under 90% RH humidity and 17°C conditions. Symptoms were observed and lesion diameter was measured at 7 dpi.

E3 Ubiquitin Ligase Activity Assay

The full-length coding sequence of *PUB13* (1,983 bp) was cloned into the pGEX-6P-1 vector, which contains a GST tag. PUB13 carrying the mutation

of Val-273 to Arg ($V^{273}R$) was generated using the QuikChange Site-Directed Mutagenesis kit (Stratagene; no. 200518) with the following primers: M1F (5′-TCGCTGGAAATGATGAGAGATCCACGTATTGTTTCATCAG-3′) and M1R (5′-CTGATGAAACAATACGTGGATCTCTCATCATTTCCAGCGA-3′). The GST-PUB13/$V^{273}R$ fusion protein was expressed in *Escherichia coli* BL21, and 1.0 μg of GST-PUB13/$V^{273}R$ was used for each reaction. Arabidopsis ubiquitin (an ubiquitin monomer of UBQ14 [At4g02890]; approximately 2.0 μg) fused with a His tag, wheat (*Triticum aestivum*) E1 (GI: 136632; approximately 40.0 ng), and human E2 (UBCH5b; approximately 40.0 ng) were used in the in vitro E3 ligase activity assays as described (Xie et al., 2002). The reaction samples were separated by 10% SDS-PAGE and detected by western blot with the nickel-horseradish peroxidase or anti-GST antibody.

Sequence data from this article can be found in the GenBank/EMBL data libraries under accession number At3g46510.

Supplemental Data

The following materials are available in the online version of this article.

Supplemental Figure S1. Amino acid comparison of the U-box domain in PUB13 and SPL11, and identification of the T-DNA mutant *pub13*.

Supplemental Figure S2. Cell death and H_2O_2 accumulation in *pub13* after high-humidity treatment.

Supplemental Figure S3. Disease resistance of *pub13* under high humidity.

Supplemental Figure S4. Defense-related gene expression and SA level in *pub13*.

Supplemental Figure S5. Flowering phenotypes of *PUB13* RNAi and complemented *pub13* plants.

Supplemental Figure S6. Flowering phenotypes of *Spl11*-complemented *pub13* transgenic plants.

Supplemental Table S1. Primers used for real-time PCR and RT-PCR.

ACKNOWLEDGMENTS

We are grateful to Drs. Xinnian Dong and Mohan Rajinikanth at Duke University for providing *sid2-2* and *pad4* seeds.

Received December 20, 2012; accepted February 27, 2012; published March 1, 2012.

LITERATURE CITED

Azevedo C, Santos-Rosa MJ, Shirasu K (2001) The U-box protein family in plants. Trends Plant Sci **6:** 354–358

Borner R, Kampmann G, Chandler J, Gleissner R, Wisman E, Apel K, Melzer S (2000) A MADS domain gene involved in the transition to flowering in *Arabidopsis*. Plant J **24:** 591–599

Bowling SA, Guo A, Cao H, Gordon AS, Klessig DF, Dong X (1994) A mutation in *Arabidopsis* that leads to constitutive expression of systemic acquired resistance. Plant Cell **6:** 1845–1857

Chinchilla D, Zipfel C, Robatzek S, Kemmerling B, Nürnberger T, Jones JD, Felix G, Boller T (2007) A flagellin-induced complex of the receptor FLS2 and BAK1 initiates plant defence. Nature **448:** 497–500

Farmer LM, Book AJ, Lee KH, Lin YL, Fu H, Vierstra RD (2010) The RAD23 family provides an essential connection between the 26S proteasome and ubiquitylated proteins in *Arabidopsis*. Plant Cell **22:** 124–142

Glazebrook J, Rogers EE, Ausubel FM (1996) Isolation of Arabidopsis mutants with enhanced disease susceptibility by direct screening. Genetics **143:** 973–982

González-Lamothe R, Tsitsigiannis DI, Ludwig AA, Panicot M, Shirasu K, Jones JD (2006) The U-box protein CMPG1 is required for efficient activation of defense mechanisms triggered by multiple resistance genes in tobacco and tomato. Plant Cell **18:** 1067–1083

Hatakeyama S, Yada M, Matsumoto M, Ishida N, Nakayama KI (2001) U box proteins as a new family of ubiquitin-protein ligases. J Biol Chem **276:** 33111–33120

Henriques R, Jang IC, Chua NH (2009) Regulated proteolysis in light-related signaling pathways. Curr Opin Plant Biol **12:** 49–56

Jang IC, Yang JY, Seo HS, Chua NH (2005) HFR1 is targeted by COP1 E3 ligase for post-translational proteolysis during phytochrome A signaling. Genes Dev **19:** 593–602

Kardailsky I, Shukla VK, Ahn JH, Dagenais N, Christensen SK, Nguyen JT, Chory J, Harrison MJ, Weigel D (1999) Activation tagging of the floral inducer *FT*. Science **286:** 1962–1965

Kawai-Yamada M, Ohori Y, Uchimiya H (2004) Dissection of *Arabidopsis* Bax inhibitor-1 suppressing Bax-, hydrogen peroxide-, and salicylic acid-induced cell death. Plant Cell **16:** 21–32

Liu LJ, Zhang YC, Li QH, Sang Y, Mao J, Lian HL, Wang L, Yang HQ (2008) COP1-mediated ubiquitination of CONSTANS is implicated in cryptochrome regulation of flowering in *Arabidopsis*. Plant Cell **20:** 292–306

Lu D, Lin W, Gao X, Wu S, Cheng C, Avila J, Heese A, Devarenne TP, He P, Shan L (2011) Direct ubiquitination of pattern recognition receptor FLS2 attenuates plant innate immunity. Science **332:** 1439–1442

Ludwig A, Tenhaken R (2000) Defence gene expression in soybean is linked to the status of the cell death program. Plant Mol Biol **44:** 209–218

Martínez C, Pons E, Prats G, León J (2004) Salicylic acid regulates flowering time and links defence responses and reproductive development. Plant J **37:** 209–217

Mosher S, Moeder W, Nishimura N, Jikumaru Y, Joo SH, Urquhart W, Klessig DF, Kim SK, Nambara E, Yoshioka K (2010) The lesion-mimic mutant *cpr22* shows alterations in abscisic acid signaling and abscisic acid insensitivity in a salicylic acid-dependent manner. Plant Physiol **152:** 1901–1913

Mudgil Y, Shiu SH, Stone SL, Salt JN, Goring DR (2004) A large complement of the predicted Arabidopsis ARM repeat proteins are members of the U-box E3 ubiquitin ligase family. Plant Physiol **134:** 59–66

Ohi MD, Gould KL (2002) Characterization of interactions among the Cef1p-Prp19p-associated splicing complex. RNA **8:** 798–815

Schwab R, Ossowski S, Riester M, Warthmann N, Weigel D (2006) Highly specific gene silencing by artificial microRNAs in *Arabidopsis*. Plant Cell **18:** 1121–1133

Staswick PE, Serban B, Rowe M, Tiryaki I, Maldonado MT, Maldonado MC, Suza W (2005) Characterization of an *Arabidopsis* enzyme family that conjugates amino acids to indole-3-acetic acid. Plant Cell **17:** 616–627

Trujillo M, Ichimura K, Casais C, Shirasu K (2008) Negative regulation of PAMP-triggered immunity by an E3 ubiquitin ligase triplet in *Arabidopsis*. Curr Biol **18:** 1396–1401

Trujillo M, Shirasu K (2010) Ubiquitination in plant immunity. Curr Opin Plant Biol **13:** 402–408

Valverde F, Mouradov A, Soppe W, Ravenscroft D, Samach A, Coupland G (2004) Photoreceptor regulation of CONSTANS protein in photoperiodic flowering. Science **303:** 1003–1006

van den Burg HA, Tsitsigiannis DI, Rowland O, Lo J, Rallapalli G, Maclean D, Takken FL, Jones JD (2008) The F-box protein ACRE189/ACIF1 regulates cell death and defense responses activated during pathogen recognition in tobacco and tomato. Plant Cell **20:** 697–719

van Wees SC, Chang HS, Zhu T, Glazebrook J (2003) Characterization of the early response of Arabidopsis to *Alternaria brassicicola* infection using expression profiling. Plant Physiol **132:** 606–617

Vega-Sánchez ME, Zeng L, Chen S, Leung H, Wang GL (2008) SPIN1, a K homology domain protein negatively regulated and ubiquitinated by the E3 ubiquitin ligase SPL11, is involved in flowering time control in rice. Plant Cell **20:** 1456–1469

Vorwerk S, Schiff C, Santamaria M, Koh S, Nishimura M, Vogel J, Somerville C, Somerville S (2007) EDR2 negatively regulates salicylic acid-based defenses and cell death during powdery mildew infections of Arabidopsis thaliana. BMC Plant Biol **7:** 35–48

Wada KC, Takeno K (2010) Stress-induced flowering. Plant Signal Behav **5:** 944–947

Wada KC, Yamada M, Shiraya T, Takeno K (2010) Salicylic acid and the flowering gene FLOWERING LOCUS T homolog are involved in poor-nutrition stress-induced flowering of Pharbitis nil. J Plant Physiol **167:** 447–452

Wang GF, Seabolt S, Hamdoun S, Ng G, Park J, Lu H (2011) Multiple roles

of WIN3 in regulating disease resistance, cell death, and flowering time in Arabidopsis. Plant Physiol **156:** 1508–1519

Wildermuth MC, Dewdney J, Wu G, Ausubel FM (2001) Isochorismate synthase is required to synthesize salicylic acid for plant defence. Nature **414:** 562–565

Wohlgemuth H, Mittelstrass K, Kschieschan S, Bender J, Weigel HJ, Overmyer K, Kangasjarvi J, Sandermann H, Langebartels C (2002) Activation of an oxidative burst is a general feature of sensitive plants exposed to the air pollutant ozone. Plant Cell Environ **25:** 717–726

Xiang T, Zong N, Zou Y, Wu Y, Zhang J, Xing W, Li Y, Tang X, Zhu L, Chai J, et al (2008) Pseudomonas syringae effector AvrPto blocks innate immunity by targeting receptor kinases. Curr Biol **18:** 74–80

Xie Q, Guo HS, Dallman G, Fang S, Weissman AM, Chua NH (2002) SINAT5 promotes ubiquitin-related degradation of NAC1 to attenuate auxin signals. Nature **419:** 167–170

Yang CW, González-Lamothe R, Ewan RA, Rowland O, Yoshioka H, Shenton M, Ye H, O'Donnell E, Jones JD, Sadanandom A (2006) The E3 ubiquitin ligase activity of *Arabidopsis* PLANT U-BOX17 and its functional tobacco homolog ACRE276 are required for cell death and defense. Plant Cell **18:** 1084–1098

Yee D, Goring DR (2009) The diversity of plant U-box E3 ubiquitin ligases: from upstream activators to downstream target substrates. J Exp Bot **60:** 1109–1121

Yin Z, Chen J, Zeng L, Goh M, Leung H, Khush GS, Wang GL (2000) Characterizing rice lesion mimic mutants and identifying a mutant with broad-spectrum resistance to rice blast and bacterial blight. Mol Plant Microbe Interact **13:** 869–876

Yu X, Klejnot J, Zhao X, Shalitin D, Maymon M, Yang H, Lee J, Liu X, Lopez J, Lin C (2007) *Arabidopsis* cryptochrome 2 completes its post-translational life cycle in the nucleus. Plant Cell **19:** 3146–3156

Zeng LR, Park CH, Venu RC, Gough J, Wang GL (2008) Classification, expression pattern, and E3 ligase activity assay of rice U-box-containing proteins. Mol Plant **1:** 800–815

Zeng LR, Qu S, Bordeos A, Yang C, Baraoidan M, Yan H, Xie Q, Nahm BH, Leung H, Wang GL (2004) Spotted leaf11, a negative regulator of plant cell death and defense, encodes a U-box/armadillo repeat protein endowed with E3 ubiquitin ligase activity. Plant Cell **16:** 2795–2808

Zhang J, Li W, Xiang T, Liu Z, Laluk K, Ding X, Zou Y, Gao M, Zhang X, Chen S, et al (2010) Receptor-like cytoplasmic kinases integrate signaling from multiple plant immune receptors and are targeted by a Pseudomonas syringae effector. Cell Host Microbe **7:** 290–301